



1 Calcification in a marginal sea – influence of seawater  $[Ca^{2+}]$  and carbonate chemistry on  
2 bivalve shell formation

3

4 Jörn Thomsen<sup>1</sup>, Kirti Ramesh<sup>1,2</sup>, Trystan Sanders<sup>1</sup>, Markus Bleich<sup>2</sup>, Frank Melzner<sup>1</sup>

5 <sup>1</sup>Marine Ecology, GEOMAR Helmholtz Centre for Ocean Research, Kiel, Germany

6 <sup>2</sup>Institute of Physiology, Christian-Albrechts-University Kiel, 24098 Kiel, Germany

7

8 Running headline: Abiotic effects on mussel calcification

9

## 10 Abstract

11 In estuarine coastal systems such as the Baltic Sea, mussels suffer from low salinity which  
12 limits their distribution. Anthropogenic climate change is expected to cause further  
13 desalination which will lead to local extinctions of mussels in the low saline areas. It is  
14 commonly accepted that mussel distribution is limited by osmotic stress. However, along the  
15 salinity gradient environmental conditions for biomineralization are successively becoming  
16 more adverse as a result of reduced  $[Ca^{2+}]$  and dissolved inorganic carbon ( $C_T$ ) availability.  
17 In larvae, calcification is an essential process starting during early development with  
18 formation of the prodissoconch I (PD I) shell which is completed under optimal conditions  
19 within 2 days.

20 Experimental manipulations of seawater  $[Ca^{2+}]$  start to impair PD I formation in *Mytilus* larvae  
21 at concentrations below 3 mM, which corresponds to conditions present in the Baltic at  
22 salinities below 8 g kg<sup>-1</sup>. In addition, lowering dissolved inorganic carbon to critical  
23 concentrations (<1 mM) similarly affected PD I size which was well correlated with calculated  
24  $\Omega_{\text{Aragonite}}$  and  $[Ca^{2+}][HCO_3^-]/[H^+]$  in all treatments. Comparing results for larvae from the  
25 western Baltic with a population from the central Baltic revealed significantly higher tolerance  
26 of PD I formation to lowered  $[Ca^{2+}]$  and  $[Ca^{2+}][HCO_3^-]/[H^+]$  in the low saline adapted  
27 population. This may result from genetic adaptation to the more adverse environmental  
28 conditions prevailing in the low saline areas of the Baltic.

29 The combined effects of lowered  $[Ca^{2+}]$  and adverse carbonate chemistry represent major  
30 limiting factors for bivalve calcification and can thereby contribute to distribution limits of  
31 mussels in the Baltic Sea.

32

## 33 Key-words

34 Baltic Sea, bivalves, calcium, calcification, carbonate chemistry, climate change

35

## 36 1. Introduction

37 Salinity is one of the most important environmental parameters limiting the distribution of  
38 aquatic species. Many marine organisms exhibit little tolerance to reduced salinity and are  
39 thus not able to thrive in brackish water environments influenced by riverine inputs (Whitfield  
40 et al. 2012). On the other hand, some animals, such as bivalves and crustaceans tolerate the  
41 dilution of the ambient seawater and are able to inhabit estuarine, brackish water habitats  
42 (Westerbom et al. 2002). However, within these habitats, organisms need to tolerate a  
43 number of environmental stressors which are changing concomitantly.

44 Generally, lowered ambient ion concentrations affect an organism's ability to maintain  
45 cellular homeostasis. In response, some organisms such as crustaceans actively regulate  
46 the ionic composition of their extracellular fluids. However, mytilid mussels do not control  
47 haemolymph osmolarity and ionic composition mostly corresponds to that of ambient  
48 seawater (Thomsen et al. 2010). Thus tissues are subjected to a diluted medium in brackish  
49 water but the inorganic composition of the intracellular space needs to be regulated in order  
50 to maintain enzymatic functions. At moderately lowered salinity, intracellular  $[K^+]$  and  $[Na^+]$   
51 are kept relatively stable at about 200 and 100 mM, respectively, but  $[K^+]$  drops rapidly under  
52 strong hypoosmotic stress to avoid cell swelling (Willmer 1978, Wright et al. 1989; Silva and  
53 Wright 1994). In order to stay iso-osmotic with their environment following long-term  
54 acclimation to lowered salinity, intracellular  $[K^+]$  and  $[Na^+]$  are maintained at lower  
55 concentrations (Willmer 1978, Natochin et al. 1979). In addition, bivalves reduce the



56 concentration of intracellular compatible organic osmolytes (Hochachka and Somero 2002)  
57 such as certain amino acids, taurine and betaine during the acclimation phase (Silva and  
58 Wright 1994, Kube et al. 2006). However, at a certain critical salinity threshold ( $S_{crit}$ ), the  
59 intracellular organic osmolyte pools are depleted which has been suggested to eventually  
60 limit species fitness (Kube et al. 2006; Podbielski et al. 2016).

61 At the same time, bivalves produce an external shell composed of  $CaCO_3$  and an organic  
62 matrix (Falini et al. 1996). The shell enables adult bivalves to live in intertidal habitats and is  
63 an effective protection against predation but shell formation has been shown to be sensitive  
64 to lowered salinity (Malone and Dodd 1967). Under favourable environmental conditions,  
65 calcification begins already in early development and the first larval shell (prodissoconch I,  
66 PD I) is completed within the first 48 hours after fertilization. PD I formation is an important  
67 prerequisite for the successful development of bivalve larvae as larvae seem to commence  
68 feeding only after completion of the shell which provides structural support (e.g. muscle  
69 attachment site) for the functional velum (Lucas and Rangel 1983; Cragg 1985). However,  
70 PD I formation is highly sensitive to chemical and environmental stressors (Williams and Hall  
71 1999) and initiation of feeding is delayed under adverse carbonate chemistry (Waldbusser et  
72 al. 2015).

73 Recently, a number of studies investigated how changes of seawater carbonate chemistry  
74 affect marine calcifiers. Those studies were mostly motivated by the ongoing input of  
75 anthropogenic  $CO_2$  into the oceans which results in a drop of pH and lowered  $[CO_3^{2-}]$ , a  
76 process called ocean acidification. Bivalve shell formation is highly sensitive to modifications  
77 of carbonate chemistry and therefore negatively affected by ocean acidification (Gazeau et al.  
78 2013; Waldbusser et al. 2014; Thomsen et al. 2015). The exact reason for the sensitivity of  
79 calcification to adverse carbonate chemistry is still under debate (Cyronak et al. 2015).  
80 Lowered saturation of seawater with respect to calcium carbonate ( $\Omega$ ,  $[Ca^{2+}][CO_3^{2-}]/K^*sp$ )  
81 (with  $K^*sp$ =stoichiometric solubility product (Mucci 1983)) could affect the kinetic of shell  
82 formation (according to  $r = k(\Omega-1)^n$  with  $r$ =mineral precipitation rate,  $k$ =rate constant and  
83  $n$ =reaction order, Waldbusser et al. 2014) and undersaturation leads to dissolution of existing  
84 calcium carbonate structures (Thomsen et al. 2010; Melzner et al. 2011, Haynert et al. 2014).  
85 Alternatively, the substrate inhibitor ratio (SIR) defined as the availability of the substrate for  
86 calcification in the form of dissolved inorganic carbon ( $C_T$ ) or  $HCO_3^-$  and the inhibitory effect  
87 of lowered seawater pH (increased  $[H^+]$ ) could restrict calcification rate (Bach 2015; Thomsen  
88 et al. 2015; Fassbender, et al. 2016).

89 Independent of the exact mode of action, larval bivalve calcification is driven by uptake of  
90 seawater  $Ca^{2+}$  and inorganic carbon ( $C_T$ ) whereas metabolic carbon is only of minor  
91 importance and contributes by less than 10 % in larvae and adults (McConnaughey and  
92 Gillikin 2008, Waldbusser et al. 2015). Oceanic  $[Ca^{2+}]$  is about 10 mM, but necessarily  
93 linearly related with seawater salinity and thus reduced in estuaries. Freshwater  $[Ca^{2+}]$  are in  
94 general much lower (<1-2 mM  $[Ca^{2+}]$ , Ohlson and Anderson 1990; Juhna and Klavins 2000).  
95 Oceanic  $C_T$  is about 2 mM whereby  $HCO_3^-$  and  $CO_3^{2-}$  contribute about 90 and 8 % to the  $C_T$   
96 pool, respectively.  $C_T$  of seawater equilibrated with the atmosphere is directly proportional to  
97 salinity as it is depending on seawater total alkalinity ( $A_T$ ). Therefore, calcifiers are facing  
98 abiotic conditions in brackish water habitats which most likely affect their ability to form a  
99 shell.

100 The Baltic Sea is an example of a brackish water habitat which is substantially influenced by  
101 precipitation and riverine input (Gustafsson et al. 2014) which results in a salinity gradient  
102 from 25 g  $kg^{-1}$  in the Kattegat transition zone to basically freshwater in the Gulfs of Riga,  
103 Finland and Bothnia. As a consequence,  $[Ca^{2+}]$ ,  $A_T$  and  $C_T$  decline linearly along the salinity  
104 gradient (Kremling and Wilhelm 1997; Beldowski et al. 2010). However, varying composition  
105 of riverine freshwater results in differing  $A_T$ -salinity correlations and in the Gulf of Riga,  $A_T$   
106 and thus  $C_T$  even increases with lowered salinity (Beldowski et al. 2010).

107 The Baltic Sea is among the coastal ecosystems which are most heavily influenced by  
108 anthropogenic activity. Eutrophication enhanced hypoxia or even anoxia events in the  
109 benthic ecosystem. As respiratory oxygen consumption is coupled to  $CO_2$  production,  
110 hypoxia is always accompanied by a pronounced increase of  $pCO_2$  and thus affects the



111 carbonate system simultaneously (Melzner et al. 2013). Furthermore, climate change is  
112 expected to increase precipitation in the Baltic catchment area which may cause increased  
113 riverine runoff leading to reduced salinity (0 - 45 % reduction) in particular in the north-  
114 eastern and central Baltic Sea (Meier et al. 2006; Gräwe et al. 2013). This shift in salinity will  
115 most likely induce a substantial retreat of the marine fauna and flora and expansion of limnic  
116 species into the formerly brackish water habitats (Johannesson et al. 2011).

117 Mytilid mussels (*Mytilus* spp.) are among the most abundant organisms of the Baltic Sea  
118 ( $10^{13}$  individuals) contributing up to 90% to local hard bottom biomass, and thus are  
119 important habitat builders (Enderlein and Wahl 2004, Johannesson et al. 2011). Their  
120 distribution along the Finish, Swedish and Estonian coast is limited by salinities of about 4.5  
121  $\text{g kg}^{-1}$  when abundance, biomass and growth drastically decline (Westerbom et al. 2002;  
122 Martin et al. 2013; Riisgard et al. 2014). As growth combines both somatic growth and shell  
123 formation, it is unclear which physiological mechanism exactly limits performance and  
124 therefore the distribution of mussels (Riisgard et al. 2014).

125 Currently, distribution limits of marine bivalves in estuaries are commonly related to the  
126 inability of intracellular osmoregulatory adjustment at lowered salinity (Maar et al. 2015).  
127 However, as  $[\text{Ca}^{2+}]$  and  $C_T$  availability decline along the Baltic Sea salinity gradient it is likely  
128 that the calcification process is negatively affected as well. This process has not been  
129 previously considered as a factor contributing to distribution limits of mussels. In this study,  
130 we investigated the effects of seawater  $[\text{Ca}^{2+}]$  independently of salinity in combination with  
131 lowered  $C_T$  availability on the calcification performance of larval *Mytilus* spp. and correlated  
132 the experimental data with environmental conditions present in the Baltic Sea.

133

## 134 2. Material and Methods

### 135 2.1 Animal collection and spawning

136 Adult mussels were collected from subtidal depths at the pier of GEOMAR in Kiel Fjord (shell  
137 length: 4-6 cm,  $54^{\circ}19.8'N$ ;  $010^{\circ}09.0'E$ ) and at the wooden groynes close to Koserow on the  
138 island of Usedom (shell length: 2-3 cm,  $54^{\circ}03.4'N$ ;  $014^{\circ}00.4'E$ ) between May and June 2016  
139 (Fig. 1). Median salinity for Kiel Fjord and Usedom, located ~350 km east of Kiel, are ~ 17  
140 and 7  $\text{g kg}^{-1}$ , respectively (Table 1).

141 Mussels in the Baltic Sea represent hybrids of *Mytilus edulis* x *trossulus* with increasing  
142 *trossulus* allele frequency towards the less saline, eastern Baltic (Stuckas et al. 2009). Thus  
143 mussels collected in Kiel represent the Baltic *M. edulis*-like and animals from Usedom belong  
144 to the *M. trossulus*-like genotype (Stuckas et al. 2017).

145 Specimens were either used for spawning immediately after collection or kept in cold storage  
146 ( $9^{\circ}\text{C}$ ) in order to delay gonad maturation for up to 3 months. Stored mussels (ca. 500 g  
147 mussel wet biomass per 20 L tank, 12 tanks) were fed 6 times a week with 500 mL of  
148 *Rhodomonas* solution (ca.  $2 \times 10^6$  cells  $\text{mL}^{-1}$ ) supplemented with a commercial bivalve diet  
149 (*Acuinuga*, Spain) and water was exchanged twice a week (Thomsen et al. 2010).  
150 *Rhodomonas* spp. were cultured in PES medium as described previously with the exception  
151 of using 40 L cylinders (Thomsen et al. 2010).

152 All experiments were performed at  $17^{\circ}\text{C}$ . Spawning was induced by exposing the animals to  
153 rapidly elevated water temperature between  $18\text{-}25^{\circ}\text{C}$  using heaters. Spawning specimens  
154 were separated from the remaining animals and eggs and sperms were collected individually  
155 in beakers filled with 0.2  $\mu\text{m}$  filtered seawater (FSW). Subsequently, eggs were pooled and  
156 fertilized with a pooled sperm solution. For the Kiel population, 5 individual experimental runs  
157 were performed with varying number of dams and sires used for crossings in each run. In  
158 total 16 dams and 18 sires were used. For the Usedom population one run with 4 replicates  
159 was performed for which gonads from 5 dams and 4 sires were pooled. Fertilization success  
160 was determined by verifying the presence of a polar body and first and second cell division of  
161 zygotes and was above 90% in all runs. Embryos (4-8 cell stage) and non-calcified  
162 trochophora (in one experimental run of the Kiel population) from all parents were transferred  
163 in equal numbers into the experimental units (volume: 25 or 50 mL in round plastic beakers)  
164 at a density of 10 embryos/larvae  $\text{mL}^{-1}$ .



165 Three days post fertilization animals were removed from the experimental units by filtering  
166 the full water volume through a filter with a mesh size of 20  $\mu\text{m}$  or by collecting larvae  
167 individually using a pipette in treatments with low survival. Subsequently, larvae were fixed  
168 using 40 % paraformaldehyde (PFA, pH 8.0) resulting in a final PFA concentration of 4%.  
169 Pictures of larvae were taken using a stereomicroscope (Leica M165 FC) equipped with a  
170 Leica DFC 310 FX camera and LAS V4.2 software. Calcification was assessed by measuring  
171 the larval shell length. PD I shell length was assessed using Image J 1.50i by measuring the  
172 maximal shell length in parallel to the hinge or the maximal shell diameter for larvae that had  
173 not developed a complete PD I shell.

174  
175

## 176 2.2 Experimental manipulation of seawater $[\text{Ca}^{2+}]$ and carbonate chemistry

177 Artificial seawater (ASW) was prepared according to Kester (1967) for salinities of 14 and 7 g  
178  $\text{kg}^{-1}$  for experiments with *M. edulis*-like and *trossulus*-like, respectively, by adding NaCl,  
179  $\text{NaSO}_4$ , KCl,  $\text{NaHCO}_3$ , KBr,  $\text{H}_3\text{BO}_3$ ,  $\text{MgCl}_2$ ,  $\text{CaCl}_2$ , and  $\text{SrCl}_2$  to deionised water.  $\text{Ca}^{2+}$  free  
180 artificial seawater (CFSW) was prepared by omitting  $\text{CaCl}_2$  and adjusting osmolarity similar to  
181 ASW by increasing NaCl concentrations.  $\text{pH}_{\text{NBS}}$  was adjusted to 8.0 using NaOH. All  
182 experimental treatments comprised 5 % of 0.2  $\mu\text{m}$  filtered seawater (FSW) from Kiel Fjord  
183 which was adjusted to salinity 7 g  $\text{kg}^{-1}$  for the Usedom population experiment to ensure that  
184 trace elements were present. The comparison of shell sizes of larvae kept in control ASW +  
185 5% FSW or 100 % FSW yielded no significant differences ( $p > 0.05$ ). Varying seawater  $[\text{Ca}^{2+}]$   
186 treatments were prepared by mixing ASW and CFSW (lowered  $[\text{Ca}^{2+}]$ ) or by addition of  $\text{CaCl}_2$   
187 from a 500 mM stock solution to ASW (elevated  $[\text{Ca}^{2+}]$ ). Following mixing, water samples  
188 were taken and seawater  $[\text{Ca}^{2+}]$  was measured using a flame photometer (EFOX 5053,  
189 Eppendorf, Germany) calibrated with urine standards (Biorapid GmbH, Germany).

190 Seawater carbonate chemistry was manipulated by increasing alkalinity by addition of  
191  $[\text{NaHCO}_3]$  to ASW or by lowering alkalinity by adding 1M HCl to the experimental units.  
192 Excess  $\text{CO}_2$  was removed by aeration of the experimental units for 30 min and embryos were  
193 only added after pH had increased again to stable values ( $\sim 7.8$ ). Seawater pH was  
194 determined on the NBS scale using a WTW 3310 pH meter equipped with a Sentix 81  
195 electrode. Seawater  $C_T$  was determined using an AIRICA  $\text{CO}_2$  analyzer and verified by  
196 measuring certified reference material (Dickson et al. 2003). Seawater carbonate system  
197 parameters ( $\text{HCO}_3^-$ ,  $\text{CO}_3^{2-}$ ,  $\Omega_{\text{aragonite}}$ ) were calculated using the CO2SYS program with  
198  $\text{KHSO}_4$ , K1 and K2 dissociation constants after Dickson et al. (1990) and Roy et al. (1993),  
199 respectively.  $\text{pH}_{\text{NBS}}$  was converted to total scale pH.  $\Omega_{\text{aragonite}}$  and  $[\text{Ca}^{2+}][\text{HCO}_3^-]/[\text{H}^+]$  were  
200 linearly adjusted according to measured seawater  $[\text{Ca}^{2+}]$  (Table 2).

201

## 202 2.3 Microelectrode measurements of $[\text{Ca}^{2+}]$ in the calcifying space of D-stage veliger

203 Using ion-selective electrodes,  $\text{Ca}^{2+}$  gradients were measured in seawater and in the  
204 calcification space (CS) below the surface of the shell in veliger larvae three days after  
205 fertilization. The experimental set up and hardware was identical to that of Stumpp et al.  
206 (2012), except for the addition of a metal plate connected to a water cooling system for  
207 temperature control.

208 Borosilicate glass capillary tubes (inner diameter 1.2 mm, outer diameter, 1.5 mm) with  
209 filament were pulled on a DMZ-Universal puller (Zeitz Instruments, Germany) to  
210 micropipettes with tip diameters of 1-3  $\mu\text{m}$ . Micropipettes were silanized with dimethyl  
211 chlorosilane (Sigma-Aldrich, USA) in an oven at 200°C for 1h. Calcium sensitive liquid ion  
212 exchangers (LIX) and LIX-PVC membranes were prepared according to de Beer et al. (2000)  
213 with  $\text{Ca}^{2+}$  ionophore II (Sigma Aldrich). The microelectrodes were back filled with a KCl based  
214 electrolyte (200 mM KCl, 2 mM  $\text{CaCl}_2 \cdot 2\text{H}_2\text{O}$ ) and thereafter front loaded with LIX and finally  
215 LIX-PVC at a length of 150  $\mu\text{m}$  and 50  $\mu\text{m}$ , respectively. To measure calcium in the CS,  
216 larvae were placed into the temperature controlled perfusion chamber mounted on an  
217 inverted microscope (Axiovert 135, Zeiss, Germany) at a density of 100  $\text{mL}^{-1}$  and were held  
218 in position using a holding pipette. The ion-selective probe was mounted on a remote-  
219 controlled micro-manipulator and was introduced beneath the shell from the side of the



220 growing edge, where stable measurements were obtained within 5-10 seconds.  
221 Microelectrode calibration was verified by measuring  $[Ca^{2+}]$  of seawater standards as  
222 described above and analogue outputs were channelled through an amplifier (WPI  
223 Instruments, USA) to a chart recorder (Gould Instruments, USA).

224

#### 225 2.4 Seawater $[Ca^{2+}]$ and carbonate chemistry of the Baltic Sea

226 Seawater  $[Ca^{2+}]$  ( $mM\ kg^{-1}$ ) was calculated for salinities between 3 and  $20\ g\ kg^{-1}$  using the  
227 correlation for chlorinities  $<4.5$  and  $>4.5\ g\ kg^{-1}$  provided by Kremling and Wilhelm (1997) and  
228 a salinity-chlorinity conversion after Millero (1984).  $[Ca^{2+}]$  was calculated for salinity values  
229 measured in Kiel Fjord (N=4250, weekly measurements 2005-2009, 0-18 m,  $54^{\circ}19.8'$  N,  
230  $10^{\circ}9.0'$  E, Clemmesen et al., unpublished, Casties et al. 2015) and at the Oder Bank  
231 (N=260,000, hourly measurements, 2000-2015, 3+12 m water depths,  $54^{\circ}4.6'$  N,  $14^{\circ}9.6'$  E,  
232  $\sim 8$  km off the *M. trossulus*-like collection site at Usedom (BSH 2000-2015, Table. 1). As  
233 distribution of mytilid bivalves is limited by salinities below  $4.5\ g\ kg^{-1}$  the calculation covers  
234 the full  $[Ca^{2+}]$  range relevant for mussels in this estuary (Westerborn et al. 2002). Carbonate  
235 chemistry calculations are based on the salinity-alkalinity correlation published by Beldowski  
236 et al. (2010) for salinities between 3 and  $20\ g\ kg^{-1}$  and a seawater surface  $pCO_2$  of  $400\ \mu atm$   
237 assuming equilibrium with current atmospheric  $CO_2$  concentrations of  $\sim 400$  ppm.  
238 Calculations were performed for seawater temperatures of  $15^{\circ}C$  which corresponds to  
239 average conditions experienced by larvae during the natural reproductive period from April to  
240 June. The Baltic Sea has four sub areas which are differentially impacted by the inflow of  
241 riverine freshwater and their respective chemical properties: the Central Baltic Sea with the  
242 Kattegat transition area, the Gulf of Riga, the Gulf of Finland and the Bothnian Sea with Gulf  
243 of Bothnia. Depending on the chemical properties of the riverine input, seawater carbonate  
244 chemistry can differ substantially for similar salinity values between the four regions. The  
245 same calculations were performed for predicting future conditions using atmospheric  $CO_2$   
246 concentration of  $800$  ppm.

247

#### 248 2.5 Statistical analysis

249 All statistical analyses (t-test, Kruskal-Wallis test followed by Dunn's test, regression analysis,  
250 linear and nonlinear model parameter fitting) were performed using R and the mosaic  
251 package. Population comparisons were performed by fitting linear models for log transformed  
252 data. Each experimental unit was considered as a replicate. Values in text and figures are  
253 replicate means  $\pm$  standard error.

254

255

### 256 **3. Results**

#### 257 3.1 PD I shell formation and CS $[Ca^{2+}]$ under varying seawater $[Ca^{2+}]$

258 Larval development until PD I formation was investigated for *M. edulis*-like collected in Kiel  
259 Fjord. The lowest seawater  $[Ca^{2+}]$  tested in the experiment was  $0.51\ mM$  which did not allow  
260 successful development of larvae to the trochophore stage in the Kiel population and was  
261 thus not considered in subsequent experiments. At all other  $[Ca^{2+}]$  treatments, early  
262 development was not adversely affected and larvae started to calcify prodissoconch I.  
263 However, at  $[Ca^{2+}]$  of  $<2\ mM$  larvae were not able to produce a complete PD I shell. Even  
264 after 7 days, shell size did not increase above a mean diameter of  $63.7 \pm 6.0\ \mu m$  although  
265 larvae stayed viable and continued to actively swim. In all other treatments, shells were fully  
266 developed within 72 h post fertilization, but shell length declined linearly at  $[Ca^{2+}]$  below  $3$   
267  $mM$  ranging between  $104.5 \pm 2.1\ \mu m$  at  $2.8\ mM$  and  $82.1 \pm 1.5\ \mu m$  at  $1.6\ mM$ , with significant  
268 reductions below  $2.5\ mM\ [Ca^{2+}]$  (H: 50.3,  $p<0.001$ , Dunn's test). Specimens kept at control  
269  $[Ca^{2+}]$  of  $4-5\ mM$  had mean lengths of  $108.2 \pm 2.5\ \mu m$ . Modifications of seawater  $[Ca^{2+}]$  in the  
270 range  $4-10\ mM$  had only minor impacts on lengths and elevated  $[Ca^{2+}]$  did not cause a  
271 further increase of shell lengths above control size (Fig. 2a, Table 3a).

271 Microelectrode measurements of  $[Ca^{2+}]$  in the CS of *M. edulis*-like revealed that CS  $[Ca^{2+}]$   
272 drops with seawater  $[Ca^{2+}]$ , (H: 21.2,  $p<0.01$ , Fig. 3a). However, larvae kept at  $3.5\ mM\ [Ca^{2+}]$   
273 (above the critical  $[Ca^{2+}]$  threshold) are characterized by CS  $[Ca^{2+}]$  of  $0.1 \pm 0.01\ mM$  above  
274 seawater concentrations (paired t-test:  $t= 16.9$ ,  $p<0.01$ , Fig. 3b). In larvae raised at  $2.6$  and



275 2.3 mM  $[\text{Ca}^{2+}]$ , the difference between seawater and CS  $[\text{Ca}^{2+}]$  declined to  $0.06 \pm 0.03$  and  
276  $0.03 \pm 0.02$  mM which was not significantly enriched compared to the ambient seawater. In  
277 contrast, the gradient between CS and seawater increased to  $0.28 \pm 0.02$  mM in larvae  
278 grown at 1.5 mM.

279 Results for shell formation rates of *M. edulis*-like larvae were compared with the *M. trossulus*-  
280 like population from Usedom. Larvae were exposed to  $[\text{Ca}^{2+}]$  between 0.4-5.8 mM (Fig. 1b,c).  
281 Overall, the response curve for *M. trossulus*-like was similar to *M. edulis*-like (Table 3b).  
282 Maximal shell sizes observed at 3.7 mM were  $120 \pm 1.5$   $\mu\text{m}$  and shell lengths started to  
283 decline at lower  $[\text{Ca}^{2+}]$ . Nevertheless, at comparable  $[\text{Ca}^{2+}]$  shell sizes were larger compared  
284 to *M. edulis*-like and larvae were able to calcify a full PD I even at 1.1 mM  $[\text{Ca}^{2+}]$  with an  
285 average size of  $81.9 \pm 3.2$   $\mu\text{m}$ . In contrast, PD I formation was not completed at 0.4 mM, yet  
286 larvae started to calcify. A linear model of the calcification response revealed a significant  
287 effect of  $[\text{Ca}^{2+}]$  and population on shell size but no interaction (Table 4a, Fig. 2c).  
288

### 289 3.2 Combined effects of seawater $[\text{Ca}^{2+}]$ and carbonate chemistry on larval calcification

290 *M. edulis*-like larvae were exposed to a range of seawater  $[\text{Ca}^{2+}]$  between 1 and 10 mM and  
291  $C_T$  concentrations between 880-3520  $\mu\text{M}$ . PD I size was not modulated by increased  
292 seawater  $C_T$  of 2900-3520  $\mu\text{M}$  compared to control conditions ( $C_T$ : 1773  $\mu\text{M}$ ) and shell length  
293 was only negatively affected by seawater  $[\text{Ca}^{2+}]$  below 3 mM (Fig. 4a). In contrast, lowered  
294 seawater  $C_T$  (975  $\mu\text{M}$ ) significantly affected shell formation and PD I length declined to  $72.5 \pm$   
295  $2.7$   $\mu\text{m}$  at control  $[\text{Ca}^{2+}]$ . Within these treatments shell length was marginally positively  
296 correlated with seawater  $[\text{Ca}^{2+}]$  but shell length remained reduced in all  $[\text{Ca}^{2+}]$  treatments  
297 (linear regression:  $63 (\pm 2.2) \mu\text{m} + 2.9 (\pm 0.7) \times [\text{Ca}^{2+}]$ ,  $F: 18.6$ ,  $p < 0.01$ ,  $R^2 = 0.47$ , Fig. 4a).  
298 Whereas, the correlation of shell length against  $[\text{Ca}^{2+}]$  under reduced  $C_T$  differed significantly  
299 from the three higher  $C_T$  treatments. Plotting PD I sizes against seawater  $\Omega_{\text{Aragonite}}$  and  
300  $[\text{Ca}^{2+}][\text{HCO}_3^-]/[\text{H}^+]$  revealed a similar correlation of calcification in all treatments (Fig. 4b, c).  
301 Calcification of larvae started to decline at  $\Omega_{\text{Aragonite}}$  below 1 with significant reductions in the  
302 treatments with  $\Omega_{\text{Aragonite}}$  below 0.5 (H: 44.5,  $p < 0.001$ , Dunn's test). Similarly, PD I size  
303 declined at  $[\text{Ca}^{2+}][\text{HCO}_3^-]/[\text{H}^+]$  values below 0.7 and shells were significantly smaller below  
304 0.3 (H: 42.5,  $p < 0.01$ , Dunn's test). In addition, the shell formation responses of *M. edulis*-like  
305 and *M. trossulus*-like to combined manipulations of  $[\text{Ca}^{2+}]$  and carbonate chemistry were  
306 more similar compared to the effects of lowered seawater  $[\text{Ca}^{2+}]$  alone (Fig. 2c, 4b,c, Table  
307 3b,c). Nevertheless, whereas the response to  $\Omega_{\text{Aragonite}}$  was similar for both hybrid populations  
308 they differed significantly in their response to  $[\text{Ca}^{2+}][\text{HCO}_3^-]/[\text{H}^+]$  (Table 4c,d).  
309

### 310 3.3 Calculation of seawater $[\text{Ca}^{2+}]$ , $\Omega$ and $[\text{Ca}^{2+}][\text{HCO}_3^-]/[\text{H}^+]$ for the Baltic Sea

311 Calculations of seawater  $[\text{Ca}^{2+}]$  were performed for the salinity range observed at the  
312 collections sites of *M. edulis*-like and *trossulus*-like in Kiel Fjord and Usedom, respectively. In  
313 Kiel Fjord, salinity fluctuated substantially between 10.5-24.7  $\text{g kg}^{-1}$  in the period 2005 – 2009  
314 which resulted in simultaneous strong variations of seawater  $[\text{Ca}^{2+}]$  between 3.6 – 7.7 mM  
315 with a mean of 5.6 mM (Table 1, Fig. 1d). In contrast, salinity in Usedom was lower with  
316 mean salinity of 7.1  $\text{g kg}^{-1}$  and, in absolute numbers, more stable (3.4-9.1  $\text{g kg}^{-1}$ , Table 1).  
317 Thus, seawater  $[\text{Ca}^{2+}]$  in Usedom was ranging between 1.5 and 3.2 mM with an average of  
318 2.7 mM (Table 1, Fig. 2d).

319 Calculation of  $[\text{Ca}^{2+}]$  along the Baltic salinity gradient revealed that the critical concentrations  
320 of 3 and 2.5 mM at which calcification is negatively affected are reached at a salinity of about  
321 7-8  $\text{g kg}^{-1}$ , respectively, in all four sub regions (Fig. 5a). In contrast, calculated values for  
322  $[\text{HCO}_3^-]/[\text{H}^+]$  are above 0.13 in almost all regions within the distribution range of mussels as  
323 long as the seawater is in equilibrium with current atmospheric  $\text{CO}_2$  concentrations (Fig. 5b)  
324 Only in the Gulf of Bothnia, critical values lower than 0.1 are observed for salinities of 4.5  $\text{g}$   
325  $\text{kg}^{-1}$  and below. For  $\Omega_{\text{Aragonite}}$ , undersaturation is observed at a salinity of 9  $\text{g kg}^{-1}$  for the  
326 central Baltic. The Gulfs of Bothnia and Finland are always undersaturated for  $\Omega_{\text{Aragonite}}$ , but  
327 the Gulf of Riga seawater is supersaturated (Fig. 5c) and strong negative effects on larval  
328 calcification can be expected for salinities of about 5  $\text{g kg}^{-1}$ . Similarly, critical values for



329  $[\text{Ca}^{2+}][\text{HCO}_3^-]/[\text{H}^+]$  of 0.3 at which PD I formation is significantly affected are reached at a  
330 salinity of  $5 \text{ g kg}^{-1}$  in most regions of the Baltic excluding the Gulf of Riga (Fig. 5d).  
331 Conditions for calcification will become more adverse in future as atmospheric  $\text{CO}_2$   
332 concentrations are going to reach 800 ppm. In this scenario, critical values for  $[\text{HCO}_3^-]/[\text{H}^+]$   
333 will be observed in most areas of Baltic at salinities below  $10 \text{ g kg}^{-1}$  (Fig. 6b). In particular,  
334  $[\text{Ca}^{2+}][\text{HCO}_3^-]/[\text{H}^+]$  and  $\Omega_{\text{Aragonite}}$  will be below the critical threshold in all areas of the Baltic  
335 Sea (Fig. 6c,d).  
336

#### 337 4. Discussion

338 This study investigated the impact of modifications of seawater  $[\text{Ca}^{2+}]$  and carbonate  
339 chemistry on shell formation of bivalve larvae. The experimental results were compared to  
340 the environmental conditions prevailing in the Baltic Sea.

341 The laboratory experiments revealed that seawater  $[\text{Ca}^{2+}]$  is a critical factor for shell  
342 formation in marine bivalves. Similarly,  $\text{Ca}^{2+}$  deposition into the shells of *Crassostrea gigas*  
343 larvae following PD I formation was similar at seawater  $[\text{Ca}^{2+}]$  of 10 and 16.8 mM but  
344 reduced by 40% at 6.1 mM (Maeda-Martinez 1987). Thus, where high oceanic  $[\text{Ca}^{2+}]$  of ~ 10  
345 mM is not limiting bivalve calcification the low concentrations present in estuaries such as the  
346 Baltic, significantly affect biomineralization.

347 In both tested populations, *M. edulis*-like and *M. trossulus*-like the overall response curve  
348 was similar and both populations become calcium limited at  $[\text{Ca}^{2+}]$  below 3 mM. *M. trossulus*-  
349 like appeared to be slightly more tolerant to lowered  $[\text{Ca}^{2+}]$  as larvae maintained larger PD I  
350 lengths at similar  $[\text{Ca}^{2+}]$  and PD I formation was successfully accomplished at 1.1 mM. The  
351 response matches seawater  $[\text{Ca}^{2+}]$  observed in the respective habitats of the tested  
352 populations and may result from either phenotypic plasticity or genetic adaptation. It is also  
353 possible that *M. edulis*-like living in the western brackish Baltic may have already adapted to  
354 lower  $[\text{Ca}^{2+}]$  compared to populations and species living in habitats characterized by higher  
355  $[\text{Ca}^{2+}]$  (Maeda-Martinez 1987). As PD I formation is a crucial but sensitive stage during larval  
356 life, impaired calcification by low  $[\text{Ca}^{2+}]$  can have significant effects on larval performance  
357 and fitness. As the distribution of bivalves is depending on successful larval dispersal, low  
358  $[\text{Ca}^{2+}]$  can be an important factor which determines the distribution limits of mussels and  
359 represents a strong selective force. Additionally, the strong  $[\text{Ca}^{2+}]$  gradient observed between  
360 the western Baltic-Kattegat transition zone and the central Baltic Sea can be one explanation  
361 for the simultaneously observed allele frequency shift from *M. edulis*-like to *trossulus*-like  
362 (Larsson et al. 2016, Stuckas et al. 2017).

363 Nevertheless, larval shell formation of Baltic mytilids starts to become  $[\text{Ca}^{2+}]$  limited at  
364 concentrations of about 3 mM and was significantly affected at 2.5 mM. Consequently, in  
365 areas of the Baltic with salinities below  $7\text{-}8 \text{ g kg}^{-1}$  and corresponding  $[\text{Ca}^{2+}] < 3 \text{ mM}$ , reduced  
366 shell formation starts to compromise overall larval performance. At the critical salinity of  $4.5 \text{ g}$   
367  $\text{kg}^{-1}$  which delineates the distribution boundary of mussels in the Baltic (Westerbom et al.  
368 2002),  $[\text{Ca}^{2+}]$  is as low as 1.8 mM whereby concentration below 2 mM substantially impaired  
369 PD I formation in our experiments. Importantly, even under these adverse conditions larvae  
370 were viable and continued active swimming for up to 7 days. Thus impaired calcification in  
371 low  $[\text{Ca}^{2+}]$  seawater can result from two mechanisms acting independently or in combination:  
372 I) continuous dissolution of existing calcium carbonate crystals under highly corrosive  
373 conditions may prevent further net calcification or II) larvae only use a pre-determined  
374 fraction of the energy stored in the egg for calcification. If this amount is not sufficient to  
375 sustain full PD I formation under low  $[\text{Ca}^{2+}]$  the budget does not seem to be adjusted to  
376 provide additional energy to complete calcification. Instead larvae do not continue  
377 calcification and may switch to an energy saving mode to stay alive. In our experiments, *M.*  
378 *trossulus*-like apparently developed a higher tolerance to low  $[\text{Ca}^{2+}]$  compared to *M. edulis*-  
379 like but incipient impairment of calcification at about 3 mM was similar in both populations  
380 which suggests relatively conserved  $[\text{Ca}^{2+}]$  transport mechanisms in both populations.

381 Impact of external  $[\text{Ca}^{2+}]$  on calcification has previously been studied mostly in corals for  
382 which a significant correlation was observed in a number of studies (e.g. Chalker 1976; Ip  
383 and Krishnaveni 1991). Whereas cytosolic calcium concentration are tightly regulated and



384 kept constantly low, calcifiers obviously developed a mechanism to accumulate high  $[Ca^{2+}]$  in  
385 specialized compartments within or outside the cell for biomineralization. In corals,  $Ca^{2+}$   
386 uptake and transport to the site of calcification is driven by a combination of diffusive and  
387 active transport and involves active transport by plasma membrane  $Ca^{2+}$ -ATPase (PMCA,  
388 Tambutte et al. 1996; Barott et al. 2015). In bivalves, calcification is performed by the outer  
389 mantle epithelium (OME) or the shell field in adults and larvae, respectively (Kniprath 1980),  
390 and a PMCA homolog has been localized in the OME of oysters and its inhibition negatively  
391 impacted shell growth in freshwater clams which might suggest a conserved function in  
392 bivalve calcification as well (Wang et al. 2008; Zhao et al. 2016).

393 Early studies suggested that the extrapallial fluid (EPF) of bivalves provides the microhabitat  
394 for calcification (Crenshaw 1972). However,  $[Ca^{2+}]$  and acid-base status of bulk EPF of adult  
395 mussels corresponds to seawater and haemolymph conditions, respectively, which supports  
396 excretion of  $CO_2$  via passive diffusion into the ambient seawater (Thomsen et al. 2010;  
397 Heinemann et al. 2012). In *M. edulis*-like larvae, kept above the critical threshold of 3 mM,  
398 CS  $[Ca^{2+}]$  was marginally but significantly elevated compared to seawater  $[Ca^{2+}]$ . At lowered  
399 environmental  $[Ca^{2+}]$  between 2-3 mM CS  $[Ca^{2+}]$  was not significantly enriched compared to  
400 seawater concentration. At these seawater  $[Ca^{2+}]$ , calcification rates were significantly  
401 reduced but larvae were still able to produce a smaller but complete PD I. At even lower  
402 ambient  $[Ca^{2+}]$  of 1.5 mM, CS  $[Ca^{2+}]$  was again significantly elevated compared to seawater  
403 which was, however, accompanied by strongly reduced PD I formation. The incapacity of  
404 larvae to maintain transmembrane  $Ca^{2+}$  transport at lowered  $[Ca^{2+}]$  potentially indicates a  
405 significant contribution of diffusion or involvement of a low affinity  $Ca^{2+}$  transporter (e.g.  
406  $Na^+/Ca^{2+}$  Exchanger) in this process (Blaustein and Lederer 1999). Thus, larvae may actively  
407 enrich CS  $[Ca^{2+}]$  to increase  $\Omega_{Aragonite}$  and support the structural integrity of the shell under  
408 corrosive conditions. Alternatively, CS  $[Ca^{2+}]$  only increased secondarily as a result of  
409 drastically reduced calcification rates.

410 In the present study, the effect of lowered  $[Ca^{2+}]$  was most pronounced under conditions  
411 when seawater carbonate chemistry was not a limiting parameter for calcification. Lowering  
412 of seawater  $C_T$ , which has a similar effect on  $\Omega_{Aragonite}$  and  $[HCO_3^-]/[H^+]$  as acidification,  
413 significantly affects the rate of PD I formation. Under these  $C_T / HCO_3^-$  limiting conditions,  
414 seawater  $[Ca^{2+}]$  had only a minor, yet slightly positive, linear effect on shell formation.  
415 Presumably the effect was smaller as  $Ca^{2+}$  uptake was not any longer the only rate limiting  
416 process but rather  $HCO_3^-$  uptake and / or  $H^+$  extrusion (Bach 2015) or impaired kinetics of  
417 crystal formation (Waldbusser et al. 2014).

418 Importantly, the applied experimental seawater manipulations of calcium and carbonate  
419 chemistry can be integrated by calculation of  $\Omega_{Aragonite}$  or extending the SIR term to  
420  $[Ca^{2+}][HCO_3^-]/[H^+]$  which also takes lowered availability of  $[Ca^{2+}]$  into account (Bach 2015;  
421 Fassbender et al. 2016). Plotting shell length against these two parameters revealed a  
422 similar response for all manipulations independent whether they were manipulated by  
423 lowered  $[Ca^{2+}]$  or  $C_T$ . The correlation of calcification with these parameters corresponded to  
424 previously observed shell formation performance of mussels and oysters resulting from  
425 modifications of seawater carbonate chemistry only (Waldbusser et al. 2014; Waldbusser et  
426 al. 2015; Thomsen et al. 2015). As salinity and temperature were not changed in the  
427 experiments performed with *M. edulis*-like  $\Omega_{Aragonite}$  and  $[Ca^{2+}][HCO_3^-]/[H^+]$  are linearly  
428 correlated and it is not possible to distinguish whether shell formation is modified by the  
429 changed kinetics of crystal formation (Waldbusser et al. 2015), higher dissolution due to  
430 undersaturation of the EPF with respect to calcium carbonate (Miller et al. 2009; Thomsen  
431 et al. 2010; Melzner et al. 2011, Frieder et al. 2017) or by lowered substrate availability and  
432 impaired  $H^+$  removal from the calcifying fluids (Thomsen et al. 2015; Bach 2015; Fassbender  
433 et al. 2016). However, the calcification response of *M. trossulus*-like was similar to *M. edulis*-  
434 like when plotted against  $\Omega_{Aragonite}$  but differed significantly for  $[Ca^{2+}][HCO_3^-]/[H^+]$  in  
435 accordance with the higher tolerance to lowered  $[Ca^{2+}]$ . This could indicate local adaptation  
436 of *M. trossulus*-like to the adverse environment in the low saline areas of the Baltic. In  
437 contrast, the response to  $\Omega_{Aragonite}$  was similar in animals from both populations which may





438 indicate that shell dissolution under corrosive conditions impacts net shell formation to the  
439 same extent.

440 Our experimental data revealed that larval calcification is substantially compromised by  
441 environmental conditions encountered in the Baltic Sea. Calculation of Baltic seawater  $[\text{Ca}^{2+}]$   
442 suggests  $[\text{Ca}^{2+}]$  limitation of calcification at salinities of about  $8 \text{ g kg}^{-1}$ . Thus, with exception of  
443 the western Baltic Sea with its higher salinity values, mussels inhabiting most areas of the  
444 Baltic suffer from low  $\text{Ca}^{2+}$  availability. Interestingly, studies measuring Baltic Sea  $[\text{Ca}^{2+}]$   
445 revealed increasing concentrations over the last decades which may have a beneficial effect  
446 on calcification for a given salinity (Kremling and Wilhelm 1997). Nevertheless, the expected  
447 overall reduction of salinity will most likely exceed the minor positive effect of  $[\text{Ca}^{2+}]$   
448 enrichment and negatively affect overall fitness by osmotic stress and secondarily  
449 calcification (Gräwe et al. 2013).

450 In contrast to  $[\text{Ca}^{2+}]$ , estimating current carbonate chemistry for the four Baltic sub regions  
451 suggests that the influence is of less importance for limitation of calcification. The calculated  
452  $[\text{HCO}_3^-]/[\text{H}^+]$  and  $\Omega_{\text{Aragonite}}$  for seawater in equilibrium with current atmospheric  $\text{CO}_2$   
453 concentrations remain above the critical thresholds of 0.1-0.13 and 1, respectively (Thomsen  
454 et al. 2015, this study). However, this conclusion does not consider the substantial variability  
455 of carbonate chemistry in the surface water of the Baltic which is modified by biogeochemical  
456 processes such as riverine composition, photosynthesis and upwelling on a seasonal and  
457 spatial scale. Seawater carbonate chemistry can be substantially modified by phytoplankton  
458 blooms in spring and early summer causing a draw down of seawater  $p\text{CO}_2$  to  $150 \mu\text{atm}$   
459 thereby causing elevated pH,  $[\text{CO}_3^{2-}]$  and  $[\text{HCO}_3^-]/[\text{H}^+]$  for several weeks (Schneider and  
460 Kuss 2004). Consequently, larvae can be exposed to environmental conditions which are  
461 beneficial for calcification. In contrast, local upwelling phenomena have the opposite effect  
462 leading to lowered pH and  $[\text{CO}_3^{2-}]$ ,  $[\text{HCO}_3^-]/[\text{H}^+]$  and elevated  $p\text{CO}_2$  (Thomsen et al. 2010;  
463 Saderne et al. 2013). Upwelling events are common in the Baltic Sea in particular along the  
464 western coastlines (Myrberg and Andrejev 2003). However, research mostly focused on the  
465 effect of upwelling on temperature and nutrient supply but neglected the local impacts on  
466 carbonate chemistry (e.g. Haapala 1994). As upwelling causes rapid elevation of  $p\text{CO}_2$  within  
467 a short period of hours but can last for several days to few weeks, thus for a significant part  
468 of a larval life time, its impact on calcification and performance of larvae can be substantial  
469 (Barton et al. 2012; Thomsen et al. 2015, 2017).

470 In addition to the present carbonate system variability, the successive increase of  
471 atmospheric  $\text{CO}_2$  concentrations and coupled pH decline in the Baltic will result in  
472 progressively adverse conditions for calcification. This process is particularly critical for  
473 mussel populations inhabiting the low saline areas of the Baltic where conditions for  
474 calcification are less favourable already today and will become more adverse in the future.  
475 Nevertheless, it has recently been shown that increasing  $A_T$  (from an unaccounted source)  
476 may partly and even completely compensate the negative effects of  $\text{CO}_2$  uptake (Müller et al.  
477 2016). Consequently, bivalve calcification may benefit from higher  $A_T$  and thus favourable  
478 carbonate chemistry in future, but lowered salinity might still affect performance.

479 Both substrates relevant for calcification,  $\text{Ca}^{2+}$  and inorganic carbon are integrated in the  
480 terms  $\Omega$  and the SIR extended to  $[\text{Ca}^{2+}][\text{HCO}_3^-]/[\text{H}^+]$ . In fact the calcification response of  
481 bivalve larvae in our experiments was accurately described by both terms for a given salinity  
482 and temperature. Nevertheless, calculations of the environmental conditions in the four Baltic  
483 sub regions revealed important differences.  $\Omega_{\text{Aragonite}}$  remains favourable for calcification ( $>1$ )  
484 in most parts of the central Baltic and in the Gulf of Riga caused by high alkaline riverine  
485 runoff and therefore prohibits dissolution of shell crystals (Juhna and Klavins 2000). In  
486 contrast, calculated values for  $[\text{Ca}^{2+}][\text{HCO}_3^-]/[\text{H}^+]$  are below the critical threshold of 0.7 in all  
487 sub regions at a salinity of  $11 \text{ g kg}^{-1}$  caused by low  $[\text{Ca}^{2+}]$ . Thus, it is of high ecological  
488 relevance whether bivalve calcification is sensitive to the reduced kinetic of shell formation  
489 and dissolution depending on  $\Omega$  or lowered substrate availability and inhibition by  $[\text{H}^+]$ .  
490 According to our experimental data most likely a combination of both parameters is  
491 determining sensitivity. However, compared to *M. edulis*-like, *M. trossulus*-like seems to have  
492 evolved a slightly higher tolerance to low  $[\text{Ca}^{2+}][\text{HCO}_3^-]/[\text{H}^+]$ , but not to low  $\Omega_{\text{Aragonite}}$ . A similar



493 response has been observed in a comparison between Baltic and North Sea mussels under  
494 simulated ocean acidification (Thomsen et al. 2017).

495 In conclusion, this study reveals strong impacts of lowered  $[Ca^{2+}]$  and carbonate chemistry,  
496 which are naturally changing along the Baltic salinity gradient, on the early calcification of  
497 mussel larvae. Strong delays and impairment of complete shell formation most likely affect  
498 the energy budget and overall physiology of mussels in the low saline areas. Consequently,  
499 low  $[Ca^{2+}]$  and adverse carbonate chemistry impact mussel fitness substantially and  
500 therefore likely seem to contribute significantly in determining the distribution of marine  
501 mussels in estuaries such as the Baltic Sea.

502

#### 503 **Author Contributions:**

504 JT conceived the study and led the writing of the manuscript; JT, KR, TS and FM collected  
505 data; JT, KR, MB, and FM analysed the data. All authors contributed to the various  
506 manuscript drafts.

507

#### 508 **Acknowledgements:**

509 The authors thank Thomas Stegmann for performing  $Ca^{2+}$  measurements, Marian Hu for  
510 supporting  $Ca^{2+}$ -microelectrode measurements and Ulrike Panknin for maintaining  
511 *Rhodomonas* cultures. Furthermore, Detlev Machoczek and Rainer Kiko are acknowledged  
512 for providing and supporting processing of Oder Bank salinity data, respectively. This study  
513 was funded by the BMBF program BIOACID subproject 2.3 and CACHE, a Marie Curie Initial  
514 Training Network (ITN) funded by the People Programme (Marie Curie Actions) of the  
515 European Union's Seventh Framework Programme FP7/2007-2013/ under REA grant  
516 agreement n°[605051]13. The authors declare no conflict of interest.

517

#### 518 **Data availability:**

519 All data are available under: Thomsen, Jörn; Ramesh, Kirti; Sanders, Trystan; Bleich, Markus;  
520 Melzner, Frank (2017): Effects of seawater calcium on calcification in mussel larvae.  
521 PANGAEA, Unpublished dataset #871804.

522

#### 523 **References:**

- 524 Bach, L.T.: The role of carbonate ion concentration for the production of calcium carbonate  
525 by marine organisms, *Biogeosciences*, 12, 4939-4951, 2015.
- 526
- 527 Barott, K.L., Perez, S.O., Linsmayer, L.B., and Tresguerres, M.: Differential localization of ion  
528 transporters suggests distinct cellular mechanisms for calcification and photosynthesis  
529 between two coral species. *Am. J. Physiol. Reg. I.*, 309, R235-R246, 2015.
- 530
- 531 Barton, A., Hales, B., Waldbusser, G.G., Langdon, C., and Felly, R.A.: The Pacific oyster  
532 *Crassostrea gigas*, shows negative correlation to naturally elevated carbon dioxide levels:  
533 Implications for near-term ocean acidification effects. *Lim. Oceanog.*, 57, 698-710, 2012.
- 534
- 535 Beldowski, J., Löffler, A., and Joensuu, L.: Distribution and biogeochemical control of total  
536  $CO_2$  and total alkalinity in the Baltic Sea. *J. Mar. Syst.*, 81, 252-259, 2010.
- 537
- 538 Blaustein, M.P., and Lederer W.J., Sodium/Calcium Exchange: Its physiological implications.  
539 *Physiological Reviews*, 79, 763-854, 1999.
- 540
- 541 BSH: Hourly meteorological observations at Station Oder Bank 2000-2015, Bundesamt für  
542 Seeschifffahrt und Hydrographie, Hamburg
- 543
- 544 Casties, I., Clemmensen, C., Melzner, F., and Thomsen, J.: Salinity dependence of  
545 recruitment success of the sea star *Asterias rubens* in the brackish western Baltic Sea.  
546 *Helgoland Mar. Res.*, 69, 169-175, 2015.
- 547



- 548 Chalker, B.E.: Calcium transport during skeletogenesis in hermatypic corals, *Comp. Biochem.*  
549 *Physiol. A*, 54, 455-459, 1976.
- 550  
551 Cragg, S.M.: The adductor and retractor muscles of the veliger of *Pecten maximus* (L.)  
552 (*Bivalvia*), *J. Mollus. Stud.*, 51, 276-283, 1985.
- 553  
554 Crenshaw, M.A.: The inorganic composition of molluscan extrapallial fluid, *Biol. Bull.*, 143,  
555 506-512, 1972.
- 556  
557 Cyronak, T., Schulz, K.G., and Jokiel, P.L.: The Omega myth: what really drives lower  
558 calcification rates in an acidifying ocean, *ICES J. Mar. Sci.*, 73, 558-562, 2015.
- 559  
560 De Beer, D., Kühl, M., Stambler, N., and Vaki, L.: A mirosensor study of light enhanced  $\text{Ca}^{2+}$   
561 uptake and photosynthesis in the reef-building hermatypic coral *Favia* sp., *Mar. Ecol. Prog.*  
562 *Ser.*, 194, 75-85, 2000.
- 563  
564 Dickson, A.G.: Standard potential of the reaction  $-\text{AgClS} + 1/2 \text{H}_2 = \text{AgS} + \text{HClAq}$  and the  
565 standard acidity constant of the ion  $\text{HSO}_4^-$  in synthetic sea-water from 273.15-K to 318.15-  
566 K, *J. Chem. Thermodyn.*, 22, 113–127, 1990.
- 567  
568 Dickson, A.G., Afghan, J.D., and Anderson, G.G.: Reference materials for oceanic  $\text{CO}_2$   
569 analysis: A method for the certification of total alkalinity. *Mar. Chem.*, 80, 185-197, 2003.
- 570  
571 Enderlein, P., and Wahl, M.: Dominance of blue mussels versus consumer-mediated  
572 enhancement of benthic diversity, *J. Sea Res.*, 51, 145-155, 2004.
- 573  
574 Falini, G., Albeck, S., Weiner, S., and Addadi, L.: Control of aragonite or calcite polymorphism  
575 by mollusk shell macromolecules, *Science*, 271, 67-69, 1996.
- 576  
577 Fassbender, A.J., Sabine, C.L., and Feifel, K.M.: Consideration of coastal carbonate  
578 chemistry in understanding biological calcification. *Geophys. Res. Lett.*, 43, 4467-4476, 2016.
- 579  
580 Frieder, C.A., Applebaum, S.L., Pan, T.C.F., Hedgecock, D., and Manahan, D.: Metabolic  
581 cost of calcification in bivalve larvae under experimental ocean acidification. *ICES J. Mar.*  
582 *Sci.*, 74, 941-954, 2017.
- 583  
584 Gazeau, F., Parker, L.M., Comeau, S., Gattuso, J.P., O'Connor, W.A., Martin, S., Pörtner, H.  
585 O., and Ross, P.M.: Impacts of ocean acidification on marine shelled molluscs. *Mar. Biol.*,  
586 160, 2207-2245, 2013.
- 587  
588 Gräwe, U., Freidland, R., and Burchard, H.: The future of the western Baltic Sea: two  
589 possible scenarios, *Ocean Dynam.*, 63, 901-921, 2013.
- 590  
591 Gustafsson, E., Wällstedt, T., Humborg, C., Mörth, C.M., and Gustafsson, B.G.: External total  
592 alkalinity loads versus internal generation: The influence of non-riverine alkalinity sources in  
593 the Baltic Sea, *Global Biochem. Cy.*, 28, 1358-1370, 2014.
- 594  
595 Haapala, J.: Upwelling and its influence on nutrient concentration in the coastal area of the  
596 Hanko Peninsula, Entrance of the Gulf of Finland, *Estuar. Coast. Shelf S.*, 38, 507-521, 1994.
- 597  
598 Haynert, K., Schönfeld, J., Schiebel, R., Wilson, B., and Thomsen, J.: Response of benthic  
599 foraminifera to ocean acidification in their natural sediment environment: a long-term  
600 culturing experiment, *Biogeosciences*, 11, 1581–1597, 2014.
- 601



- 602 Heinemann, A., Fietzke, J., Melzner, F., Böhm, F., Thomsen, J., Garbe-Schönberg, D. and  
603 Eisenhauer, A.: Conditions of *Mytilus edulis* extracellular body fluids and shell composition in  
604 a pH-treatment experiment: Acid-base status, trace elements and  $\delta^{11}\text{B}$ , *Geochem. Geophys.*  
605 *Geosy.*, 13, Q01005, 2013.
- 606  
607 Ip, Y.K., and Krishnaveni, P.: Incorporation of Strontium ( $^{90}\text{Sr}^{2+}$ ) into the skeleton of the  
608 hermatypic coral *Galaxea fascicularis*, *J. Exp. Zool.*, 258, 273-276, 1991.
- 609  
610 Johannesson, K., Smolarz, K., Grahn, M., and Andre, C.: The Future of Baltic Sea  
611 Populations: Local Extinction or Evolutionary Rescue? *AMBIO*, 40, 179-190, 2011.
- 612  
613 Juhna, T., and Klavins, M.: Water-quality changes in Latvian and Riga 1980-2000:  
614 Possibilities and Problems, *AMBIO*, 30, 306-314, 2001.
- 615  
616 Kester, D.R., Duedall, I.W., Connors, D.N., and Pytkowicz, R.M.: Preparation of artificial  
617 seawater, *Limnol. Oceanogr.*, 12, 176-179, 1967.
- 618  
619 Kniprath, E.: Larval development of the shell and the shell gland in *Mytilus* (Bivalvia). *Roux's*  
620 *Arch. Dev. Biol.*, 188, 201-204, 1980.
- 621  
622 Kremling, K., and Wilhelm, G.: Recent increase of the calcium concentrations in Baltic Sea  
623 waters. *Mar. Pollut. Bull.*, 34, 763-767, 1997.
- 624  
625 Kube, S., Gerber, A., Jansen, J.M. and Schiedek, D.: Patterns of organic osmolytes in two  
626 marine bivalves, *Macoma baltica*, and *Mytilus* spp., along their European distribution, *Mar.*  
627 *Biol.*, 149, 1387-1396, 2006.
- 628  
629 Lucas, A., and Rangel, C.: Detection of the first larval feeding in *Crassostrea gigas* using the  
630 epifluorescence microscope, *Aquaculture*, 30, 369-374, 1983.
- 631  
632 Maar, M., Saurel, C., Landes, A., Dolmer, P., and Petersen, J.K.: Growth potential of blue  
633 mussels (*M. edulis*) exposed to different salinities evaluated by a Dynamic Energy Budget  
634 model, *J. Mar. Sys.*, 148, 48-55, 2015.
- 635  
636 Maeda-Martinez, A.N.: The rates of calcium deposition in shells of molluscan larvae, *Comp.*  
637 *Biochem. Physiol. A*, 86, 21-28, 1987.
- 638  
639 Malone, P.G., and Dodd, J.R.: Temperature and salinity effects on calcification rate in *Mytilus*  
640 *edulis* and its paleoecological implications, *Limnol. Oceanogr.*, 12, 432-436, 1965.
- 641  
642 Martin, G., Kotta, J., Möller, T., and Herkül, K.: Spatial distribution of marine benthic habitats  
643 in the Estonian coastal sea, northeastern Baltic Sea. *Est. J. Ecol.*, 62, 165-191, 2013.
- 644  
645 McConnaughey T.A., and Gillikin, D.P.: Carbon isotopes in mollusk shell carbonates, *Geo-*  
646 *Mar. Lett.*, 28, 287-299, 2008.
- 647  
648 Meier, H.E.M., Kjellström, E., and Graham, L.P.: Estimating uncertainties of projected Baltic  
649 Sea salinity in the late 21st century, *Geophys. Res. Lett.*, 33, L15705, 2006.
- 650  
651 Melzner, F., Stange, P., Trübenbach, K., Thomsen, J., Casties, I., Panknin, U., Gorb, S., and  
652 Gutowska, M.A.: Food supply and seawater  $\text{pCO}_2$  impact calcification and internal shell  
653 dissolution in the Blue Mussel *Mytilus edulis*, *PLOS ONE*, 6, e24223, 2011.
- 654



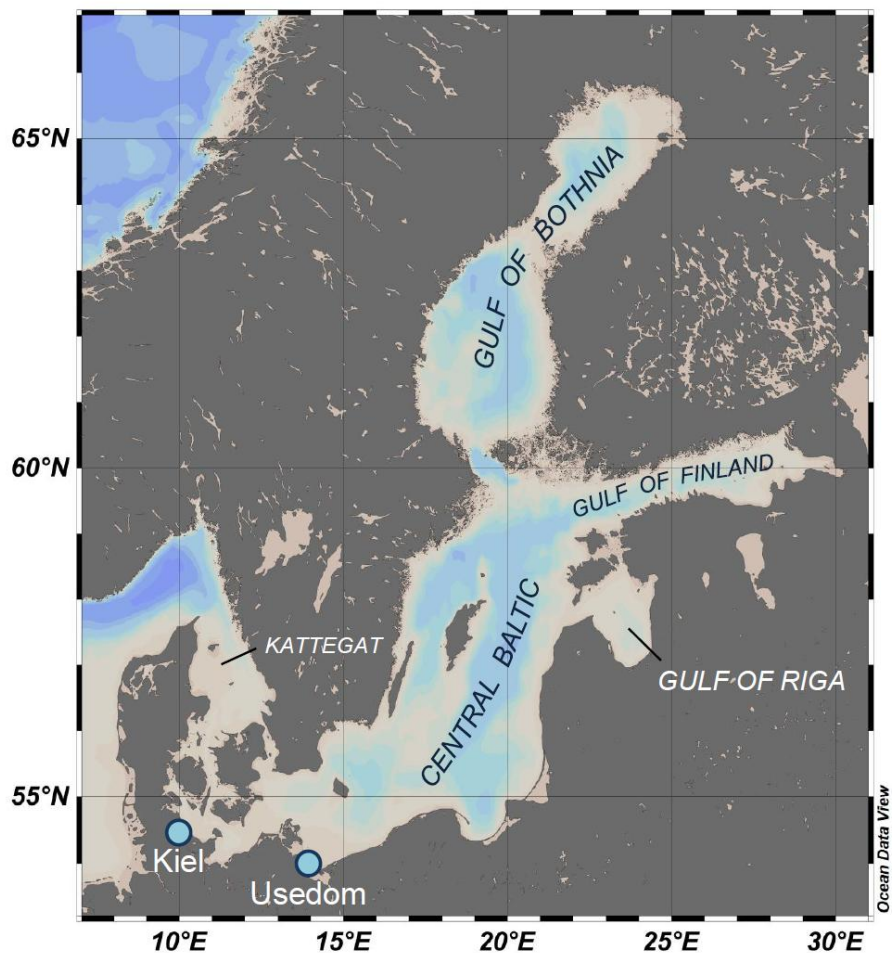
- 655 Melzner, F., Thomsen, J., Koeve, W., Oschlies, A., Gutowska, M.A., Bange, H. W., Hansen,  
656 H.P., and Körtzinger, A.: Future ocean acidification will be amplified by hypoxia in coastal  
657 habitats, *Mar. Biol.*, 160, 1875-1888, 2013.  
658
- 659 Miller, A.W., Reynolds, A.C., Sobrino, C., and Riedel, G.F.: Shellfish face uncertain future in  
660 high CO<sub>2</sub> world: Influence of acidification on oyster larvae calcification and growth in  
661 estuaries, *PLOS ONE*, 4, e5661, 2009.  
662
- 663 Millero, F.: The conductivity-density-salinity-chlorinity relationships for estuarine water,  
664 *Limnol. Oceanogr.*, 29, 1317-1321, 1984.  
665
- 666 Mucci, A.: The solubility of calcite and aragonite in seawater at various salinities,  
667 temperatures, and one atmosphere total pressure. *Am. J. Sci.*, 28, 780-799, 1983.  
668
- 669 Müller, J., Schneider, B., and Rehder, G.: Long-term alkalinity trends in the Baltic Sea and  
670 implications for CO<sub>2</sub>-induced acidification, *Limnol. Oceanogr.*, 61, 1984-2002, 2016.  
671
- 672 Myrberg, K., and Andrejev, O.: Main upwelling regions in the Baltic Sea - a statistical analysis  
673 based on three-dimensional modelling, *Boreal Environ. Res.*, 8, 97-112, 2003.  
674
- 675 Natchin, Y.V., Berger, V.Y., Khlebovich, V.V., Lavrova, E.A., and Michailova, O.Y.: The  
676 participation of electrolytes in adaptation mechanisms of intertidal molluscs' cells to altered  
677 salinity. *Comp. Biochem. Physiol A*, 63, 115-119, 1979.  
678
- 679 Ohlson, M., and Anderson, L.: Recent investigation of total carbonate in the Baltic Sea:  
680 changes from the past as a result of acid rain? *Mar. Chem.*, 30, 259-267, 1990.  
681
- 682 Podbielski, I., Bock, C., Lenz, M., and Melzner, F.: Using the critical salinity ( $S_{crit}$ ) concept to  
683 predict invasion potential of the anemone *Diadumene lineata* in the Baltic Sea, *Mar. Biol.*,  
684 163, 227, 2016.  
685
- 686 Riisgard, H.U., Larsen, P. S., Turja, R., and Lundgreen, K.: Dwarfism of blue mussels in the  
687 lower saline Baltic Sea – growth to the lower salinity limit, *Mar. Ecol. Prog. Ser.*, 517, 181-  
688 192, 2014.  
689
- 690 Roy, R.N., Roy, L.N., Vogel, K.M., Porter-Moore, C., Pearson, T., Good, C.E., Millero, F. J.,  
691 and Campbell, D.: The dissociation constants of carbonic acid in seawater at salinities 5 to  
692 45 and temperatures 0 to 45°C. *Mar. Chem.*, 44, 249-267, 1993.  
693
- 694 Saderne, V., Fietzek, P., and Herman, P.M.J.: Extreme variations of pCO<sub>2</sub> and pH in a  
695 macrophyte meadow of the Baltic Sea in summer: Evidence of the effect of photosynthesis  
696 and local upwelling, *PLOS ONE*, 8, e62689, 2013.  
697
- 698 Schneider, B., and Kuss, J.: Past and present productivity of the Baltic Sea inferred from  
699 pCO<sub>2</sub> data. *Cont. Shelf Res.*, 24, 1611-1622, 2004.  
700
- 701 Silva, A.L. and Wright, S.H.: Short-term cell volume regulation in *Mytilus californianus* gill, *J.*  
702 *Exp. Biol.*, 194, 47-68, 1994.  
703
- 704 Stuckas, H., Knobel, L., Schade, H., Breusing, C., Hinrichsen, H.-H., Bartel, M., Langguth, K.  
705 and Melzner, F.: Combining hydrodynamic modelling with genetics: Can passive larval  
706 drift shape the genetic structure of Baltic *Mytilus* populations? *Mol. Ecol.*, 26, 2765-2782,  
707 2017.  
708



- 709 Stumpp, M., Hu, M., Casties, I., Saborowski, R., Bleich, M., Melzner, F., and Dupont, S.:  
710 Digestion in sea urchin larvae impaired under ocean acidification, *Nature Clim. Change*, 3,  
711 1044-1049, 2013.
- 712  
713 Tambutte, E., Allemand, D., Mueller, E. & Jaubert, J.: A compartmental approach to the  
714 mechanism of calcification in hermatypic corals. *J. Exp. Biol.*, 199, 102-1041 1996.
- 715  
716 Thomsen, J., Gutowska, M.A., Saphörster, J., Heinemann, A., Trübenbach, K., Fietzke, J.,  
717 Hiebenthal, C., Eisenhauer, A., Körtzinger, A., Wahl, M., and Melzner, F.: Calcifying  
718 invertebrates succeed in a naturally CO<sub>2</sub>-rich coastal habitat but are threatened by high  
719 levels of future acidification, *Biogeosciences*, 7, 3879–3891, 2010.
- 720  
721 Thomsen, J., Haynert, K., Wegner, K. M., and Melzner, F.: Impact of seawater carbonate  
722 chemistry on the calcification of marine bivalves, *Biogeosciences*, 12, 4209-4220, 2015.
- 723  
724 Thomsen, J., Stapp, L.S., Haynert, K., Schade, H., Danelli, M., Lannig, G., Wegner, K.M.,  
725 and Melzner, F.: Naturally acidified habitat selects for ocean acidification-tolerant mussels,  
726 *Sci. Adv.*, 3, e1602411, 2017.
- 727  
728 Waldbusser, G.G., Brunner, E.L., Haley, B.A., Hales, B., Langdon, C.J., and Prah, F. G.: A  
729 developmental and energetic basis linking larval oyster shell formation to acidification  
730 sensitivity, *Geophys. Res. Lett.*, 40, 1–6, 2013.
- 731  
732 Waldbusser, G.G., Hales, B., Langdon, C.J., Haley, B.A., Schrader, P., Brunner, E.L., Gray,  
733 M.W., Miller, C.A., and Gimenez, I.: Saturation-state sensitivity of marine bivalve larvae to  
734 ocean acidification, *Nature Clim. Change*, 5, 273-280, 2014.
- 735  
736 Waldbusser, G.G., Hales, B., Langdon, C.J., Haley, B.A., Schrader, P., Brunner, E.L., Gray,  
737 M.W., Miller, C.A., Gimenez, I., and Hutchinson, G.: Ocean acidification has multiple modes  
738 of action in bivalve larvae, *PLOS ONE*, 10, e0128376, 2015.
- 739  
740 Wang, X., Fan, W., Xie, L., and Zhang, R.: Molecular cloning and distribution of a plasma  
741 membrane calcium ATPase homolog from the pearl oyster *Pinctada fucata*, *Tsinghua Sci.*  
742 *Technol.*, 13, 439-446, 2008.
- 743  
744 Westerborn, M., Kilpi, M., and Mustonen, O.: Blue mussels, *Mytilus edulis*, at the edge of the  
745 range: population structure, growth and biomass along a salinity gradient in the north-eastern  
746 Baltic Sea, *Mar. Biol.*, 140, 991-999, 2002.
- 747  
748 Whitfield, A.K., Elliott, M., Basset, A., Blaber, S.J.M., and West, R.J.: Paradigms in estuarine  
749 ecology – A review of the Remane diagram with a suggested revised model for estuaries,  
750 *Estuar. Coast. Shelf S.*, 97, 78-90, 2012.
- 751  
752 Williams, E.K., and Hall, J.A.: Seasonal and geographic variability in toxicant sensitivity of  
753 *Mytilus galloprovincialis*, *Australas. J. Ecotox.*, 5, 1-10, 1999.
- 754  
755 Willmer, P.G.: Sodium fluxes and exchange pumps: Further correlates of osmotic conformity  
756 in the nerves of an estuarine bivalve (*Mytilus edulis*). *J. Exp. Biol.*, 77, 207-223, 1978).
- 757  
758 Wright, S.H., Moon, D.A., and Silva, A.L.: Intracellular Na<sup>+</sup> and the control of amino acid  
759 fluxes in the integumental epithelium of a marine bivalve, *J. Exp. Biol.*, 142, 293-310, 1989.
- 760  
761 Zhao, L., Schöne, B.R., and Mertz-Kruas, R.: Delineating the role of calcium in shell  
762 formation and elemental composition of *Corbicula fluminea* (Bivalvia), *Hydrobiologica*, 790,  
763 259-270, 2016.



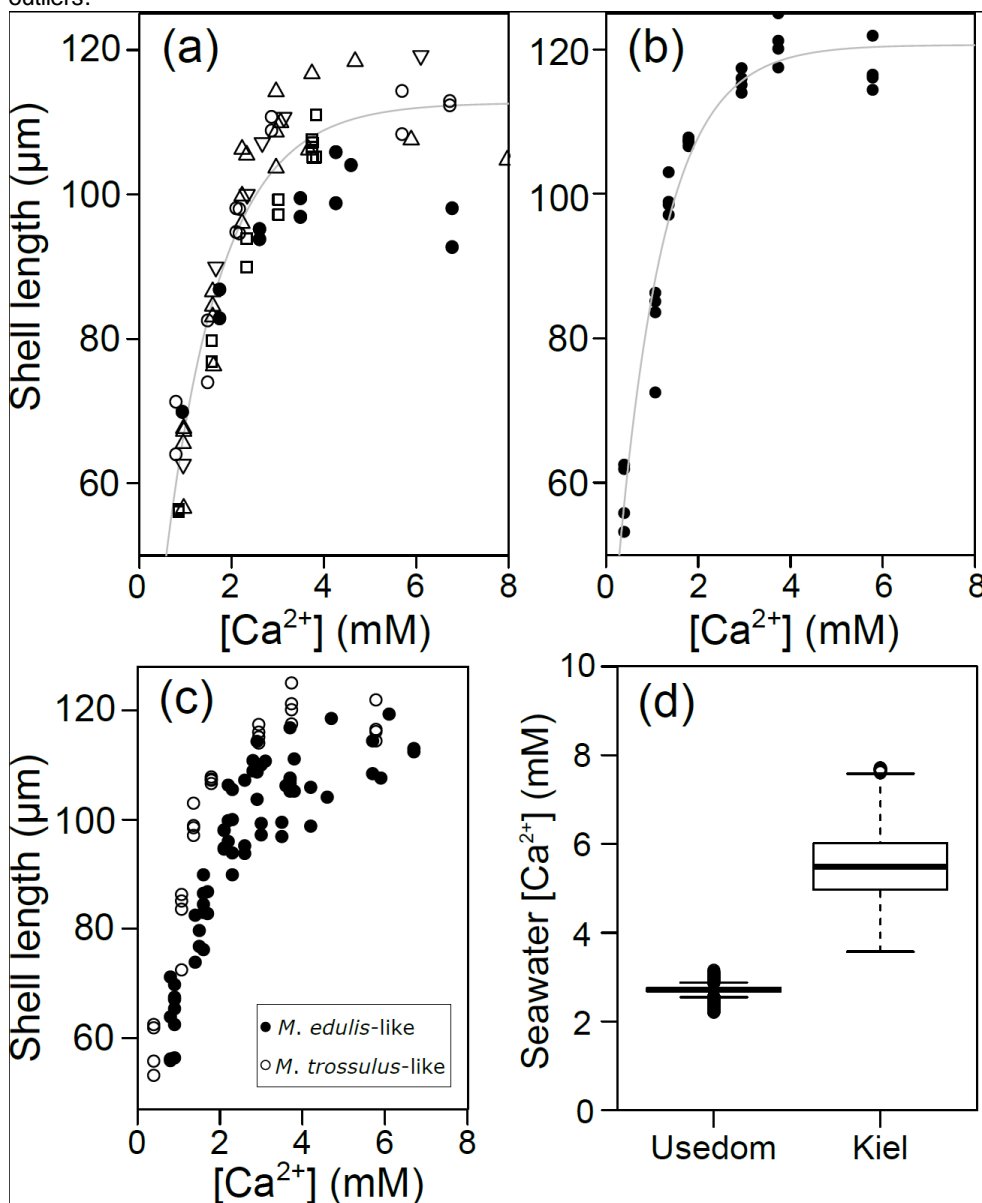
764 Fig. 1 Bathymetric map of the Baltic Sea and its sub regions which are characterized by  
765 specific carbonate chemistry. Sampling spots for mussel populations used in the experiments  
766 are indicated by light blue dots.



767  
768  
769  
770  
771  
772  
773  
774  
775  
776  
777  
778  
779  
780  
781  
782



783 Fig. 2 Prodissoconch I length of mussel larvae as a function of seawater  $[Ca^{2+}]$ . A) *M. edulis*-  
784 like, different symbols represent different experimental runs (1-5) B) *M. trossulus*-like, C)  
785 Comparison of *M. edulis*-like and *trossulus*-like, D) Boxplots of seawater  $[Ca^{2+}]$  at the  
786 collection site in Kiel Fjord and at Usedom depicting median, 25 and 75% quartiles and  
787 outliers.

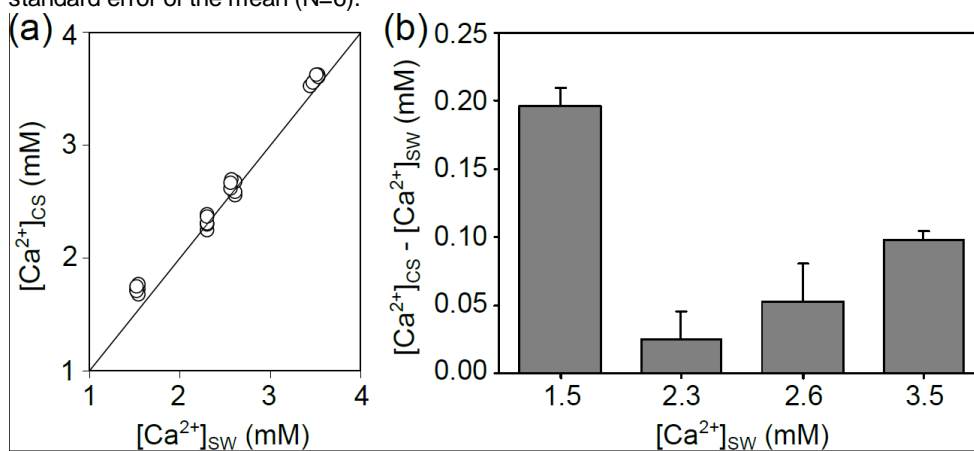


788  
789  
790  
791  
792  
793  
794





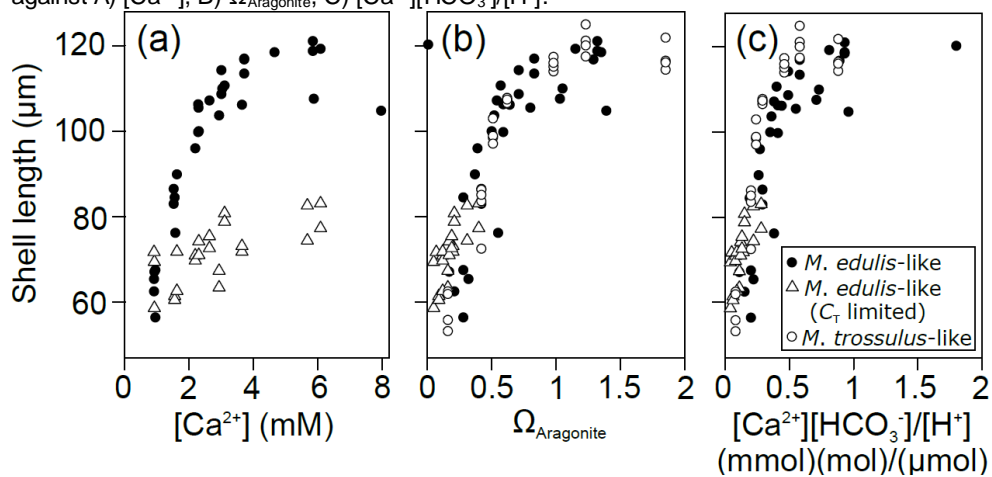
795 Fig. 3 [Ca<sup>2+</sup>] in the calcifying space (CS) of *M. edulis*-like larvae. A) CS [Ca<sup>2+</sup>] as a function of  
796 seawater [Ca<sup>2+</sup>], the line indicates the isoline B) Difference between CS [Ca<sup>2+</sup>] and seawater  
797 [Ca<sup>2+</sup>] at four [Ca<sup>2+</sup>] treatments expressed as [Ca<sup>2+</sup>]<sub>CS</sub>-[Ca<sup>2+</sup>]<sub>sw</sub>. Bar chart depicts mean ±  
798 standard error of the mean (N=6).



799  
800  
801  
802  
803  
804  
805  
806  
807  
808  
809  
810  
811  
812  
813  
814  
815  
816  
817  
818  
819  
820  
821  
822  
823  
824  
825  
826  
827  
828  
829  
830  
831  
832  
833



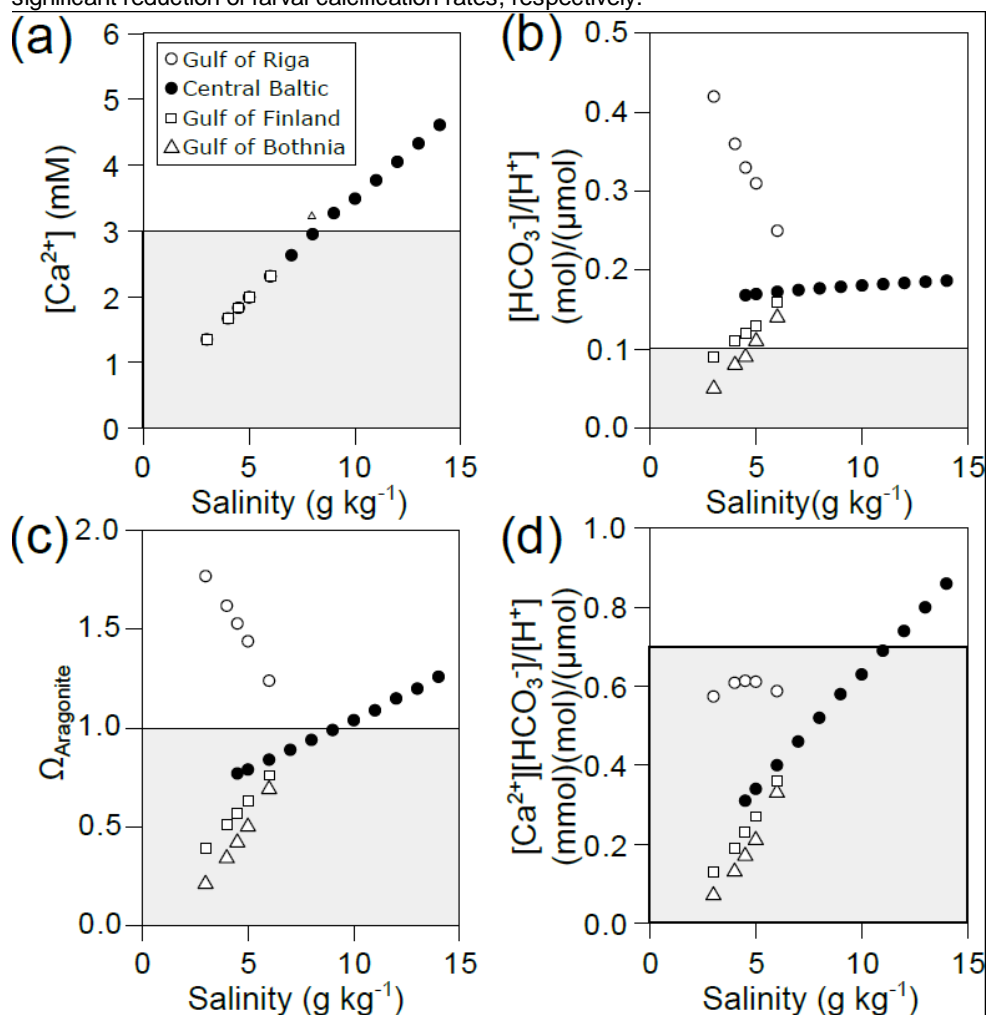
834 Fig. 4 Prodissoconch I length of mussel larvae exposed to varying  $C_T$  and  $[Ca^{2+}]$  plotted  
835 against A)  $[Ca^{2+}]$ , B)  $\Omega_{Aragonite}$ , C)  $[Ca^{2+}][HCO_3^-]/[H^+]$ .



836  
837  
838  
839  
840  
841  
842  
843  
844  
845  
846  
847  
848  
849  
850  
851  
852  
853  
854  
855  
856  
857  
858  
859  
860  
861  
862  
863  
864  
865  
866  
867  
868  
869  
870  
871  
872



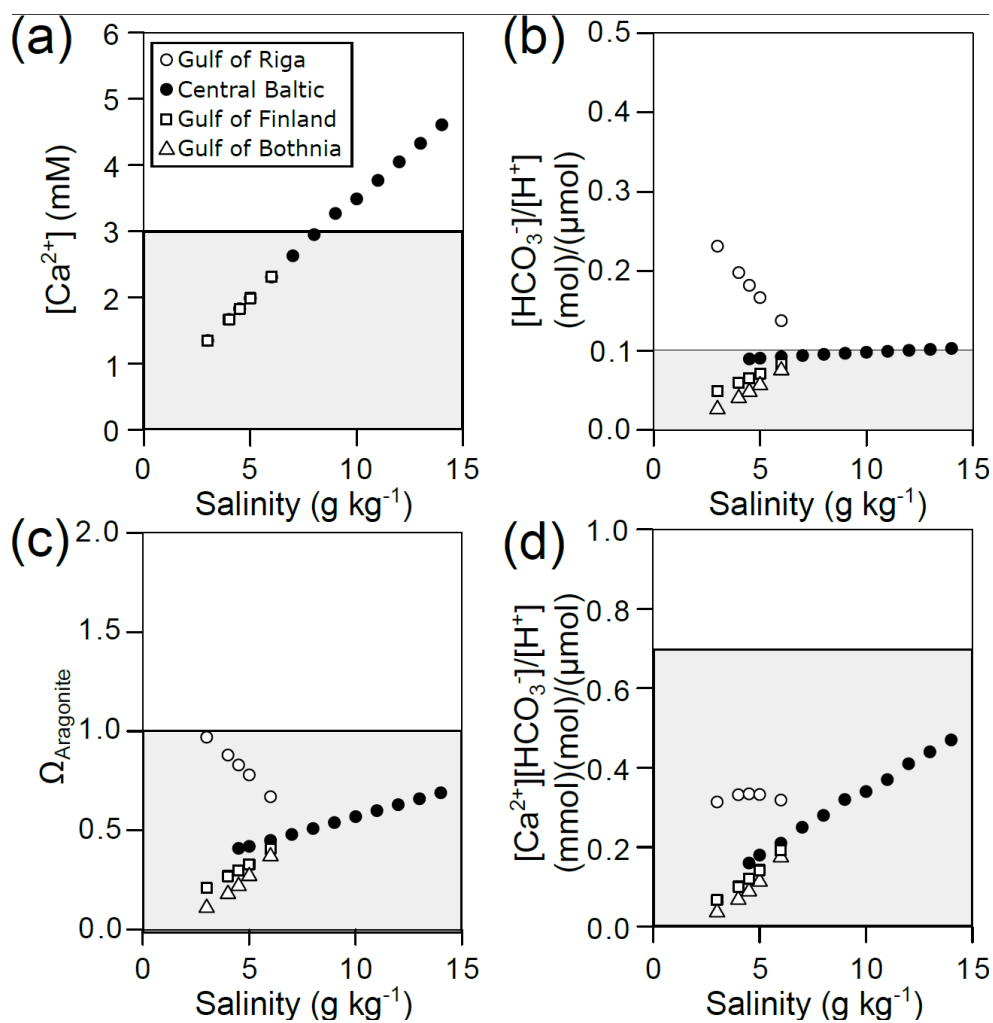
873 Fig. 5 Environmental parameters relevant for calcification in the Baltic Sea calculated for  
874 current salinity- $A_T$  correlations and atmospheric  $CO_2$  concentration (400 ppm). A)  $[Ca^{2+}]$ , B)  
875  $[HCO_3^-]/[H^+]$ , C)  $\Omega_{Aragonite}$  and D)  $[Ca^{2+}][HCO_3^-]/[H^+]$  plotted against salinity for the four sub  
876 regions of the Baltic Sea. Dashed lines and grey areas indicate conditions of incipient and  
877 significant reduction of larval calcification rates, respectively.



878  
879  
880  
881  
882  
883  
884  
885  
886  
887  
888  
889  
890  
891  
892



893 Fig. 6 Predicted environmental parameters relevant for calcification in the Baltic Sea  
894 calculated for current salinity- $A_T$  correlations and future atmospheric  $CO_2$  concentration (800  
895 ppm). A)  $[Ca^{2+}]$ , B)  $[HCO_3^-]/[H^+]$ , C)  $\Omega_{Aragonite}$  and D)  $[Ca^{2+}][HCO_3^-]/[H^+]$  plotted against salinity  
896 for the four sub regions of the Baltic Sea. Dashed lines and grey areas indicate conditions of  
897 incipient and significant reduction of larval calcification rates, respectively.  
898



899  
900  
901  
902  
903  
904  
905  
906  
907  
908  
909  
910  
911  
912



913 Table 1. Natural variability of salinity and [Ca<sup>2+</sup>] in Kiel Fjord and Usedom.

914

Salinity (g kg <sup>-1</sup> )	Usedom	Kiel
Min.	3.44	10.50
1st Qu.	6.81	15.30
Median	7.19	17.10
Mean	7.14	17.15
3rd Qu.	7.74	18.90
Max.	9.33	24.70

[Ca <sup>2+</sup> ] (mM)	Usedom	Kiel
Min.	2.22	3.57
1st Qu.	2.67	4.97
Median	2.71	5.49
Mean	2.70	5.51
3rd Qu.	2.75	6.01
Max.	3.14	7.70

915

916

917

918

919

920

921

922

923

924

925

926

927

928

929

930

931

932

933

934

935

936

937

938

939

940

941

942

943

944

945

946

947

948

949

950

951



952 Table 2: Experimental conditions during larval experiments, N:1-10 determinations,  $\Omega_{\text{Aragonite}}$   
 953 and  $[\text{Ca}^{2+}][\text{HCO}_3^-]/[\text{H}^+]$  are calculated from measured  $[\text{Ca}^{2+}]$ ,  $C_T$  and  $\text{pH}_{\text{NBS}}$ .

A)  $[\text{Ca}^{2+}]$  manipulation experiments with *M. edulis*-like

treatment	$[\text{Ca}^{2+}]$ (mmol/L)
<1 mM	$0.86 \pm 0.02$
1.5 - 2 mM	$1.56 \pm 0.03$
2.0 - 2.5 mM	$2.19 \pm 0.03$
2.5 - 3 mM	$2.82 \pm 0.05$
3.0 - 4.0 mM	$3.62 \pm 0.06$
4.0 - 5.0 mM	$4.42 \pm 0.11$
5.0 - 6.0 mM	$5.74 \pm 0.07$
6.0 - 8.0 mM	$6.83 \pm 0.25$
>8.0 mM	$9.22 \pm 0.10$

B)  $[\text{Ca}^{2+}]$  manipulation experiments with *M. trossulus*-like

treatment	$[\text{Ca}^{2+}]$ (mmol/L)	$\Omega_{\text{Aragonite}}$	$[\text{Ca}^{2+}][\text{HCO}_3^-]/[\text{H}^+]$ [mmol][mol]/[ $\mu\text{mol}$ ]
<1 mM	$0.40 \pm 0.02$	$0.16 \pm 0.02$	$0.08 \pm 0.01$
1 mM	$1.07 \pm 0.04$	$0.43 \pm 0.00$	$0.20 \pm 0.01$
1-1.5 mM	$1.36 \pm 0.00$	$0.51 \pm 0.03$	$0.24 \pm 0.01$
1.5 - 2 mM	$1.79 \pm 0.03$	$0.62 \pm 0.04$	$0.29 \pm 0.02$
2.5 - 3 mM	$2.94 \pm 0.03$	$0.98 \pm 0.07$	$0.46 \pm 0.03$
3.0 - 4.0 mM	$3.74 \pm 0.04$	$1.23 \pm 0.06$	$0.58 \pm 0.03$
>5.0 mM	$5.78 \pm 0.01$	$1.86 \pm 0.11$	$0.88 \pm 0.04$

C)  $[\text{Ca}^{2+}]$  and carbonate systems manipulation experiments with *M. edulis*-like

treatment	$[\text{Ca}^{2+}]$ (mmol/L)	$\Omega_{\text{Aragonite}}$	$[\text{Ca}^{2+}][\text{HCO}_3^-]/[\text{H}^+]$ [mmol][mol]/[ $\mu\text{mol}$ ]
control + high $C_T$	$0.93 \pm 0.02$	$0.26 \pm 0.07$	$0.18 \pm 0.05$
	$1.55 \pm 0.03$	$0.45 \pm 0.09$	$0.31 \pm 0.06$
	$2.25 \pm 0.06$	$0.64 \pm 0.15$	$0.44 \pm 0.10$
	$2.99 \pm 0.05$	$0.80 \pm 0.22$	$0.55 \pm 0.15$
	$3.69 \pm 0.04$	$1.05 \pm 0.23$	$0.73 \pm 0.16$
	$5.45 \pm 0.70$	$1.36 \pm 0.04$	$0.94 \pm 0.02$
	$8.69 \pm 1.03$	2.63	1.8
low $C_T$	$0.92 \pm 0.01$	$0.06 \pm 0.01$	$0.04 \pm 0.01$
	$1.59 \pm 0.05$	$0.10 \pm 0.03$	$0.07 \pm 0.02$
	$2.25 \pm 0.08$	$0.14 \pm 0.03$	$0.10 \pm 0.02$
	$2.78 \pm 0.21$	$0.17 \pm 0.02$	$0.12 \pm 0.01$
	$3.37 \pm 0.38$	$0.20 \pm 0.01$	$0.14 \pm 0.01$
	$5.88 \pm 0.29$	$0.36 \pm 0.06$	$0.25 \pm 0.05$

954  
 955  
 956  
 957  
 958



959 Table 3: Model parameters (a, b, c) describing PD I size as a function of experimental  
 960 seawater conditions for *Mytilus edulis*-like and *trossulus*-like: Shell length ( $\mu\text{m}$ ) =  $a + b \cdot$   
 961  $e^{(c \cdot [\text{parameter}])}$ .

A) Seawater $[\text{Ca}^{2+}]$				
<i>M. edulis</i> -like	Estimate	std Error	t-value	p
a	112.7	1.8	63.4	<0.001
b	-100.7	7.6	-13.3	<0.001
c	-0.8	0.1	-9.3	<0.001
<i>M. trossulus</i> -like				
	Estimate	std Error	t-value	p
a	120.6	1.8	66	<0.001
b	-94.5	5.2	-18.1	<0.001
c	-1	0.1	-10.3	<0.001
B) Seawater $\Omega_{\text{Aragonite}}$				
<i>M. edulis</i> -like	Estimate	std Error	t-value	p
a	118.9	3.8	31.1	<0.001
b	-106.1	16.1	-6.6	<0.001
c	-3.1	0.6	-4.7	<0.001
<i>M. trossulus</i> -like				
	Estimate	std Error	t-value	p
a	121.6	2.3	53.5	<0.001
b	-100.8	6.4	-15.7	<0.001
c	-2.8	0.3	-9.0	<0.001
C) Seawater $[\text{Ca}^{2+}][\text{HCO}_3^-]/[\text{H}^+]$				
<i>M. edulis</i> -like	Estimate	std Error	t-value	p
a	125.9	5.0	25.3	<0.001
b	-73.5	4.3	-17.2	<0.001
c	-1.8	0.3	-5.9	<0.001
<i>M. trossulus</i> -like				
	Estimate	std Error	t-value	p
a	121.4	2.2	54.0	<0.001
b	-104.8	7.1	-14.9	<0.001
c	-6.0	0.7	-9.0	<0.001

962  
 963  
 964  
 965  
 966  
 967  
 968  
 969  
 970  
 971  
 972  
 973  
 974  
 975  
 976  
 977  
 978  
 979  
 980  
 981  
 982



983 Table 4: Results for linear models fitted on log transformed data of shell length and seawater  
 984 parameters, significant results in bold.

A) Response to  $[\text{Ca}^{2+}]$

	Estimate	std Error	t-value	p
<b>Intercept</b>	<b>4.17</b>	<b>0.07</b>	<b>59.2</b>	<b>&lt;0.001</b>
<b>Ca<sup>2+</sup></b>	<b>0.31</b>	<b>0.06</b>	<b>4.9</b>	<b>&lt;0.001</b>
<b>population</b>	<b>0.12</b>	<b>0.04</b>	<b>2.8</b>	<b>&lt;0.01</b>
Ca <sup>2+</sup> :population	-0.01	0.04	-0.3	>0.05
F: 82.1		p: <0.001		R2: 0.77

B) Response to  $\Omega_{\text{Aragonite}}$

	Estimate	std Error	t-value	p
<b>Intercept</b>	<b>4.64</b>	<b>0.05</b>	<b>90.4</b>	<b>&lt;0.001</b>
<b><math>\Omega_{\text{Aragonite}}</math></b>	<b>0.13</b>	<b>0.04</b>	<b>3.08</b>	<b>&lt;0.01</b>
population	0.04	0.03	1.23	>0.05
<b><math>\Omega_{\text{Aragonite}}</math>: population</b>	<b>0.1</b>	<b>0.03</b>	<b>2.86</b>	<b>&lt;0.01</b>
F: 116.4		p:<0.001		R2: 0.82

C) Response to  $[\text{Ca}^{2+}][\text{HCO}_3^-]/[\text{H}^+]$  (CHH)

	Estimate	std Error	t-value	p
<b>Intercept</b>	<b>4.69</b>	<b>0.08</b>	<b>60.1</b>	<b>&lt;0.001</b>
<b>CHH</b>	<b>0.27</b>	<b>0.07</b>	<b>3.8</b>	<b>&lt;0.001</b>
<b>population</b>	<b>0.13</b>	<b>0.05</b>	<b>2.5</b>	<b>&lt;0.05</b>
CHH: population	0.02	0.04	0.5	>0.05
F: 67.4		p: <0.001		R2: 0.78

985